Bio-Design and Manufacturing (2022) 5:210–219
https://doi.org/10.1007/s42242-021-00173-0

RESEARCH ARTICLE

A 3D-printed microfluidic gradient concentration chip for rapid antibiotic-susceptibility testing

Huilin Zhang[1,2,3,4] · Yuan Yao[2,4] · Yue Hui[2,4] · Lu Zhang[2,3] · Nanjia Zhou[2,4] · Feng Ju[2,3,4]

Received: 28 July 2021 / Accepted: 25 October 2021 / Published online: 24 November 2021

Abstract

The rise of antibiotic resistance as one of the most serious global public health threats has necessitated the timely clinical diagnosis and precise treatment of deadly bacterial infections. To identify which types and doses of antibiotics remain effective for fighting against multi-drug-resistant pathogens, the development of rapid and accurate antibiotic-susceptibility testing (AST) is of primary importance. Conventional methods for AST in well-plate formats with disk diffusion or broth dilution are both labor-intensive and operationally tedious. The microfluidic chip provides a versatile tool for evaluating bacterial AST and resistant behaviors. In this paper, we develop an operationally simple, 3D-printed microfluidic chip for AST which automatically deploys antibiotic concentration gradients and fluorescence intensity-based reporting to ideally reduce the report time for AST to within 5 h. By harnessing a commercially available, digital light processing (DLP) 3D printing method that offers a rapid, high-precision microfluidic chip-manufacturing capability, we design and realize the accurate generation of on-chip antibiotic concentration gradients based on flow resistance and diffusion mechanisms. We further demonstrate the employment of the microfluidic chip for the AST of *E. coli* to representative clinical antibiotics of three classes: ampicillin, chloramphenicol, and kanamycin. The determined minimum inhibitory concentration values are comparable to those reported by conventional well-plate methods. Our proposed method demonstrates a promising approach for realizing robust, convenient, and automatable AST of clinical bacterial pathogens.

Keywords Microfluidics · Gradient concentration chip · Digital light processing · Antibiotic-susceptibility test · Bacteria

Introduction

The invention and medical use of antibiotics have saved countless lives and extended the human lifespan by approximately 10 years [1]. However, the overuse and abuse of antibiotics (e.g., as animal-growth promoters) have stimulated the development and spread of antibiotic resistance in bacteria [2, 3], leading to increased challenges in treating deadly human bacterial infections. The World Health Organization and the United Nations Environment Programme have repeatedly raised alarms about the antibiotic resistance of bacteria as one of the largest threats to global health in the twenty-first century [4]. Optimizing antibiotic usage (e.g., selection and dosage) in clinical treatments based on a minimum inhibitory concentration (MIC) determined from antibiotic-susceptibility testing (AST) is considered of great importance for lowering mortality rates caused by antibiotic resistance [2].

Common AST methods based on broth dilution and disk diffusion identify changes in the turbidity of culture media by measuring optical density (OD) or the inhibition zones on agar plates [5, 6]. While these methods have been widely used in clinical tests, food safety, and environmental monitoring, they are often labor-intensive and relatively expensive. Most importantly, they involve tedious manual operations and are time consuming (e.g., because of operations such as

✉ Nanjia Zhou
zhounanjia@westlake.edu.cn

✉ Feng Ju
jufeng@westlake.edu.cn

1 College of Environmental & Resource Sciences, Zhejiang University, Hangzhou 310058, China

2 Key Laboratory of Coastal Environment and Resources of Zhejiang Province, School of Engineering, Westlake University, Hangzhou 310024, China

3 Institute of Advanced Technology, Westlake Institute for Advanced Study, Hangzhou 310024, China

4 Key Laboratory of 3D Micro/Nano Fabrication and Characterization of Zhejiang Province, Hangzhou 310024, China

culture plating and dilution). Recently, microfluidic technology has been widely used in biology to simplify and automate these processes, enabling the use of a convenient platform for small-volume, automated, high-throughput, and precise liquid control [7]. These advantages have spurred efforts to develop various microfluidic chips for bacteria testing, such as optical [8], electrochemical [9], and magnetic chips [10]. Specifically for bacterial AST, microfluidic chips provide the capability of manipulating fluids for the generation of a concentration gradient without the tedious dilution steps used in the standard 96-well plates [11].

For robust AST, it is important to control the fluid to generate a precisely controlled, antibiotic concentration gradient. Microfluidics-based methods and devices have considerable advantages (e.g., easy control and high throughput) for generating the desired concentration levels [12]. The most widely used methods include tree-shaped networks, diffusion, and the microfluidic droplet [13]. Tree-shaped networks based on mono-phase methods are widely used. Generally, in these networks, two inlets are designed: one for the reagent with the high concentration and the other for the diluted reagent. The adjacent branch channels combine and mix reagents at each stage to yield one additional stream with a different concentration based on the splitting ratios [14]. Despite its simple design, this method is limited by its relatively large device footprint, its shearing, and its propensity for easy channel clogging [13, 15]. A diffusion-based microfluidic chip is usually fabricated with two channels, i.e., a source channel and a sink channel. The concentration gradient changes gradually and typically reaches stability within 20 min [16]. Kim et al. [17] presented a diffusion-based gradient concentration chip used for rapid AST with optical image acquisition and analysis. However, the continuous areas along the channels failed to react independently, which can result in an inaccurate estimation of the MIC values [16]. Microfluidic droplets may overcome the aforementioned limitations of the tree-shaped network and diffusion methods by forming independent droplets to avoid cross-contamination. The high-throughput generation of droplets encapsulating bacteria employs a flow-focusing microfluidic chip, and a broad range of the antibiotic concentration gradient is obtained by adjusting its flow rate [18]. However, yielding stable droplets hosting the same number of bacterial cells is challenging [8, 19]. Thus, current methods for generating a precisely controlled antibiotic concentration gradient still face one or more limitations such as a large footprint, inaccurate concentration, and complex control.

In contrast to tree-shaped chips, continuous diffusion chips, and droplet chips, the droplet-trapping system is a promising method for generating both gradient concentration and isolated chambers by trapping the liquid based on two-phase flow [20]. In brief, liquids with an initially high concentration of reagents are injected which become trapped in the chambers, followed by the injection of a dilution buffer, which mixes with the reagent droplets to form different concentrations. The number of chambers is adjustable, from several to hundreds. The generated concentration can also be controlled by changing the initial concentration. This system enables flexibly controlled, high-throughput, and independent chambers, which represent a platform for AST in a large dynamic range of gradient concentrations [21, 22]. In this study, we developed a novel, 3D-printed microfluidic gradient concentration chip (μGCC) and combined it with resazurin-based bacterial metabolism assays to realize a rapid antibiotic-susceptibility test in 5 h (Fig. 1a). Resazurin is a useful and minimally toxic fluorescent dye for tracing bacteria cell metabolism and is commonly used for rapid AST [21]. The employment of digital light processing (DLP) 3D-printing technology which has been widely used for fabricating complex microfluidic chips due to its rapid printing speed, simple operation, and low equipment cost [23, 24] provides an efficient fabrication of microfluidic chips, compared with conventional photolithography [25].

This paper reports on (i) the design and fabrication of a DLP-printed microfluidic chip, (ii) the antibiotic gradient concentration-generating mechanisms, and (iii) the techniques used for trapping and storing independent droplets, and optimization for stable and adjustable concentrations of antibiotics. As a demonstration, we used the DLP-printed chip for assessing the susceptibility of *E. coli* MG1655 to three antibiotics, which allowed for a rapid and accurate determination of MIC levels comparable to those reported for the conventional 96-well plating method. The morphological changes of *E. coli* cell-size subject to different types and concentrations of antibiotics were observed and the cell phenotype changes were examined.

Material and methods

Preparation of biochemical reagents and antibiotic stocks

Phosphate-buffered saline (PBS, 10 mM, pH 7.4; Sinopharm Chemical Reagent Co., Ltd., Shanghai, China) was used to prepare the reaction solutions. Bovine serum albumin (BSA) from Macklin (Shanghai, China) was prepared in PBS (1.0%, w/v). Ampicillin sodium salt was obtained from Solarbio (Beijing, China), and kanamycin sulfate and chloramphenicol were obtained from Macklin (Shanghai, China). Ampicillin (5%, w/w) was prepared in a saturated $NaHCO_3$ solution, kanamycin (5%, w/w) was prepared in deionized water (18.2 MΩ·cm, Millipore, MA, USA), and chloramphenicol (5%, w/w) was prepared in ethanol. All these solutions were stored at − 20 °C. The antibiotic stock solutions were stored at 4 °C after sterilization by filtration (0.2 μm).

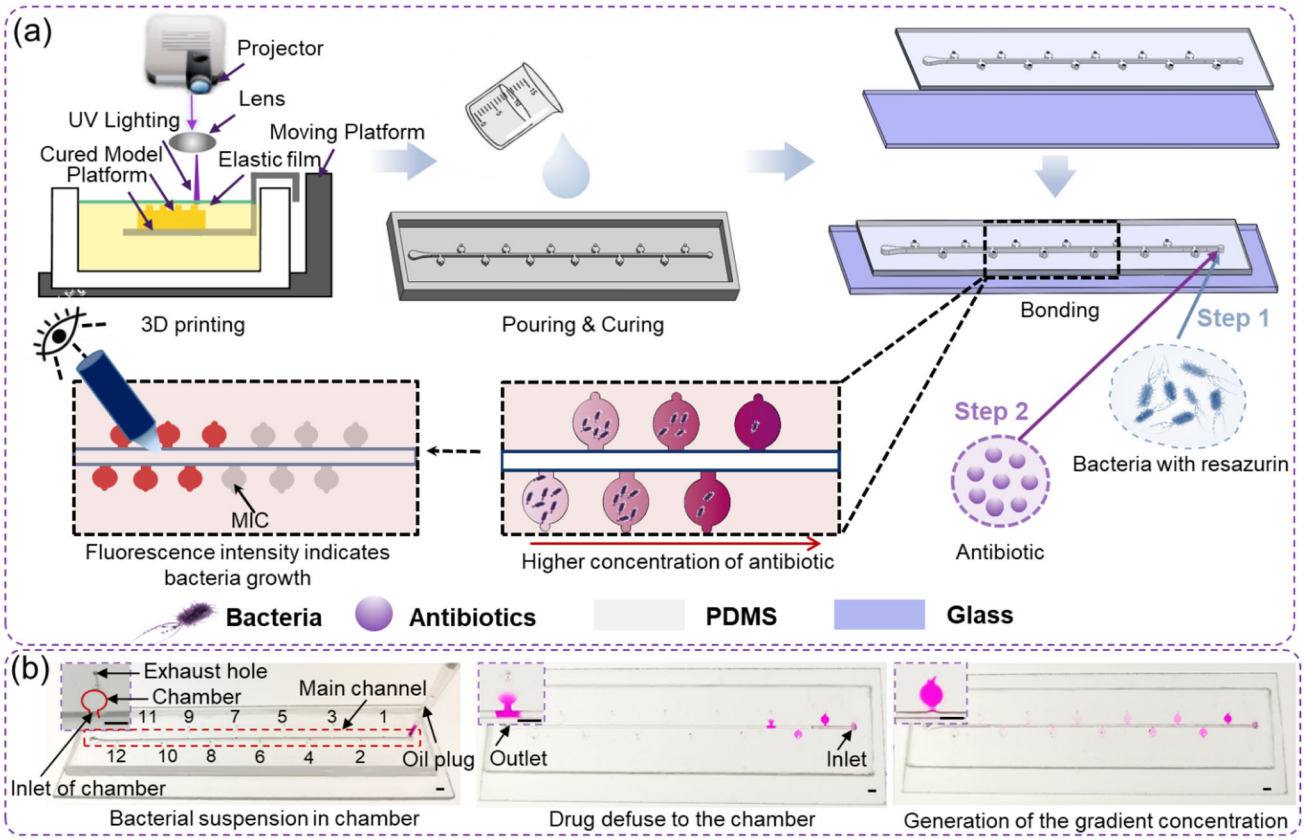

Fig. 1 Schematic showing the design and application of a 3D-printed microfluidic gradient concentration chip (μGCC) for AST of bacteria. **a** 3D printing of the microfluidic chip and the process of AST for bacteria; **b** the process of generating gradient concentration in the chip—the top left in each picture represents the enlargement of the chambers in different processes (scale bar: 2 mm)

Preparation of bacterial cell cultures

To verify the utility of the chip design, *E. coli* MG1655 was used as the model bacteria. They were revived by streaking on Luria–Bertani (LB) agar plates and cultured in LB broth at 37 °C at 180 r/min for 14–18 h to achieve an estimated concentration of about 10^9 CFU/mL (colony-forming unit per milliliter). The cultured bacteria were then serially tenfold diluted with LB broth for testing antibiotic susceptibility. For cell enumeration, 100 μL of serially tenfold-diluted cultures (with sterile PBS) was plated onto LB agar plates. The plates were incubated at 37 °C for 22–24 h, and the visible colonies were counted.

3D printing using digital light processing

The microfluidic gradient concentration chip is the crucial component of the proposed AST system (Fig. 1). The mold was initially designed and patterned on a platform with 95 layers of 3D geometry with a 40 μm thickness using the well-established soft lithography technology. We modified the original design by scaling up its thickness to 3.8 mm. It was later created by the DLP process (Fig. 1). A commercial 3D printer (nanoArch® S140, Shenzhen, China) was used in this study. It was able to fabricate the model with high-precision (printing accuracy in the z-direction: 10–40 μm) and in a larger-format (length: 94 mm, width: 52 mm, height: 45 mm) based on Projection Micro Litho Stereo Exposure [26]. In this study, we chose the "mode stitch" mode, which is for printing large models (length > 19.2 mm and/or width > 10.8 mm). In this process, the resin layer with 40 μm between the cured model platform and the elastic film was cured by UV light. The pre-designed 3D geometry was achieved by repeating this process in a layer-by-layer manner.

Design and fabrication of the gradient concentration chip

The microfluidic gradient concentration chip (μGCC) was designed based on the flow-resistance principle to avoid cross-contamination among droplets hosting different concentrations of antibiotics, so that bacterial droplets could be isolated and trapped in each of the chambers [27]. The gradient concentration chip was fabricated using polydimethylsiloxane (PDMS). The printed model was washed

and air-dried using ethanol and nitrogen, respectively. Then, the surface of the printed model was coated with Ease Release 200, a thin release agent (Mann Release Technologies, Pennsylvania, USA). Homogeneous PDMS and a curing agent from Dow Coring (Sylgard 184, Midland, the USA) were fully mixed at a ratio of 10:1 (w/w) using a stirrer (ARE-310, Thinky, Japan) at 2000 r/min for 1 min. After PDMS was fully cured at 80 °C for 2 h, the first cured PDMS was discarded as it could not be bonded well with the glass because of the effect of the release agent. The next cured PDMS with a surface oxygen plasma (PCE-6, Shenzhen, China) treatment at 29.6 W for 30 s could be bonded to a glass slide with a size of 75 mm × 25 mm × 2 mm and kept in 80 °C for 0.5 h for further stabilization. Finally, the microfluidic chip was blocked with a 1% BSA solution for 30 min before starting the AST assay.

For the AST application, the left image of Fig. 1b shows the microfluidic chip with a size of 72.5 mm × 22 mm × 3 mm, composed of the main channel, the inlet (the radius of the inlet: $R_i = 0.5$ mm) for injecting the bacterial culture, the outlet, and 12 independent chambers (labeled 1 through 12 from inlet to outlet, the radius of the chambers: $R_c = 0.8$ mm) evenly distributed on both sides of the main channel for trapping the liquid that was considered the droplet in the chambers with about 1.5 μL volume. The height of the main channel and chambers was 0.8 mm. Twelve exhaust holes were set (the radius of the exhaust hole: $R_e = 0.3$ mm) at the top of each chamber. In the liquid-loading process, each chamber and the main channel were first filled with the reaction solution. The small exhaust hole could facilitate fluid filling and restrain further fluid movement in the chamber, as there was much larger flow resistance in it than in the main channel [21, 28]. After this, a pipette was used to remove the solution in the main channel, leaving independent droplets trapped in discrete chambers.

Generation of the gradient concentration

The on-chip antibiotic-susceptibility tests were designed to be performed in 12 independent chambers with gradient concentrations of antibiotics. To visualize the gradient profiles, we used rhodamine B (MW: 479.0 g/mol), a dye with a molecular weight similar to the selected antibiotics (MW: 371.4 g/mol, 323.1 g/mol and 582.6 g/mol for ampicillin, chloramphenicol, and kanamycin, respectively) and PBS to simulate and visualize the process of generating the antibiotic gradient concentrations on the chip. Fifty microliters of PBS solution were injected into the chip to fill the main channel and the chambers. After this, the liquid in the main channel was immediately removed using a pipette (Video S1 in Supplementary Information). After generating the independent droplets in each chamber, 0.5 μL rhodamine B was injected in two-plug formulation with oil. The usage of oil was to assist the movement of rhodamine B. The two-plug solution was created using a 10 μL pipette. 2.5 μL of mineral oil was first loaded with the pipette set to 2.5 μL. Next, the pipette set wheel was turned from 2.5 to 3 μL when the pipette tip was dipped into the rhodamine B solution (Video S2 in Supplementary Information). Rhodamine B would diffuse into each of the chambers as soon as it flowed through the inlet of the chamber and touched the droplet. The concentration of rhodamine B would decrease as it flowed through from chamber 1 to chamber 11; then, the plug of rhodamine B was retained in the main channel, and chamber 12 could be set as a blank. Thus, the gradient concentration in the chamber could be generated (Video S3 in Supplementary Information). This process was conducted using a pipette to avoid using a complex instrument and a timer to help the operator control the diffusion time. The process could also be automatically controlled by the pump. Finally, droplets were taken from the exhaust holes in the chamber. The absorbance value of the liquid in each chamber was measured using Nanodrop OneC at 554 nm, and the concentration of droplets in each of the chambers was calculated based on the standard curve between absorbance and the concentration of rhodamine B. The concentration gradient of antibiotics was generated using the same, aforementioned protocol.

The on-chip antibiotic-susceptibility test

Before each AST assay, the chip was washed with 75% ethanol for sterilization, and then, the channel was covered with 1% sterile BSA for blocking. The on-chip AST was started by injecting 50 μL of LB broth bacterial suspension with resazurin (R7017, Sigma, the USA) that would be trapped by the chambers. After removing the excess liquid in the main channel, the two-plug, composed of 0.5 μL of antibiotic and 2.5 μL of mineral oil, was injected into the main channel using the pipette, and the antibiotic began to diffuse into the bacterial suspension through the chamber inlet as soon as the antibiotic flowed through each of chambers. Then, the antibiotic was gradually diffused into eleven chambers one by one. It was stopped in the main channel between chamber 11 and chamber 12 to make chamber 12 blank. Finally, all of the holes in the chip were tapped and covered by a wet paper towel to avoid evaporation of the culture medium. Cells in the captured droplets were then cultured for 5 h at 37 °C with a constant humidity (60%). The fluorescence image of each chamber could be taken by a motorized fluorescence microscope (Ni-E, Nikon, Japan; 4 × objective lens), focusing on the surface of the chambers. The excitation/emission maxima for resazurin were 490/635 nm, and the exposure time was 500 ms. The fluorescence intensity of each chamber was determined by ImageJ.

Antibiotic-susceptibility test

To validate the results of on-chip AST developed by this study, a gold-standard broth microdilution test was performed by preparing three antibiotics with a range of concentrations (1280, 640, 320, 160, 80, 40, 20, 10, 5, 2.5, 1.25, and 0 mg/L). A 180 μL volume of bacterial suspension with a final inoculum concentration of about 5×10^5 CFU/mL was pipetted into each microwell of a 96-well plate. Then, 20 μL of each prepared antibiotic suspension was added to each well. Bacteria were incubated in the presence of antibiotics for 24 h at 37 °C, and OD_{600} values were recorded using a microplate reader (Varioskan LUX, Thermo Fisher, Waltham, MA, the USA) to determine the initial bacterial concentration.

Cell morphological observation

The design of the exhaust holes also provides a convenient method for taking a sample out from the chip for conducting downstream analysis. After culturing for 5 h, the bacterial suspension in each chamber could be aspirated using a pipette from the exhaust hole and then dropped on a glass slide to inspect bacterial cell morphology using a microscope (Olympus, CX23, Japan; 40 × objective lens).

Results and discussion

Simulation of the microfluidic gradient concentration chip with trapped droplets

To better understand the fluid characteristics, we performed a fluidic, dynamic simulation of flow velocity using COMSOL 5.2. The results showed that when the radius of the exhaust hole was not smaller than the outlet ($R_1 \geq R_0$), it was difficult to fill the following chambers as the fluid leaked from the first exhaust hole (Figs. 2a and 2b). Therefore, the size of the exhaust hole should be smaller than the outlet. Further, when the liquid remaining in the main channel was removed, the solutions in each chamber and in the main channel were separated. In addition, the width of chamber inlet had an important effect on the process of the liquid filling into the chamber. Generally, a larger shear stress would be required to generate the independent droplets within different chambers with the increase in width. In this case, there was a loss of the solution that was trapped in the chambers (Fig. 2c). When the width of the chamber inlet was reduced from about 0.8 to about 0.4 mm, the volume of the trapped droplets in the chambers increased. However, the volume did not obviously change when the width of chamber inlet further decreased down to 0.4 mm. Additionally, when the width was larger than that of the main channel, it better promoted the diffusion of antibiotics. Thus, 0.5 mm was selected as an optimal width for the chamber inlet.

Optimization of on-chip gradient concentration

Rhodamine B was used as the reporter dye for modeling the gradient concentration of antibiotics with similar molecular weights and diffusion characteristics on the microfluidic chip [29]. The concentration of different antibiotics in the chambers was modeled by measuring the absorbance value change of rhodamine B. Different concentrations of rhodamine B, from 1 to 500 mg/L, were prepared on the chip, and their absorbance was detected using Nanodrop OneC (Thermos Fisher, MA, the USA). The absorbance value (A) was found to show a strong linear relationship ($A = 0.0529C_0 - 0.004$, $R^2 = 0.9983$) with the concentration of rhodamine B (C_0) in the examined concentration range.

To determine an appropriate initial concentration of antibiotic to generate the concentration gradients, we used two concentration levels of rhodamine B to simulate the results. Rhodamine B concentrations of 0.5% and 1% (w/w) were tested with a diffusion time of 30 s, generating a final concentration gradient of 1.3–265.8 mg/L and 3.7–369.2 mg/L, respectively (Fig. 3b). Rhodamine B of 0.5% (w/w) was chosen as the initial concentration to generate the concentration gradient. When the time for rhodamine B to diffuse into each of the chambers was 20 s, the final range of concentration was from 1.8 mg/L to 217.0 mg/L. When the diffusion time was increased to 30 s and 40 s, the final range of concentration became 1.3–265.8 mg/L and 1.5–338.0 mg/L, respectively. Considering both time consumption and final gradient concentration, we chose 30 s as the diffusion time.

Optimization of resazurin concentration

Resazurin was used to indicate metabolic activities of bacterial cells under exposure to antibiotics. It can be converted to resorufin with high fluorescence based on bacterial metabolism and growth [21]. However, resazurin had a slight reduction reaction and exhibits background fluorescence, even in the absence of bacterial metabolism [27]. A proper concentration of resazurin needed to be determined in this study. Therefore, five different concentrations of resazurin were tested (2, 1, 0.8, 0.6, and 0.4 mg/L). In the positive group, resazurin with five different concentrations was added into the bacterial suspension with an initial inoculum concentration of about 5×10^5 CFU/mL. As a control, a culture medium with five concentrations of resazurin was also tested. After culturing for 5 h, the fluorescence intensity of each test was observed on the chip using a motorized fluorescence microscope and measured using ImageJ. As expected, both in the positive and in the control, the fluorescence intensity increased when the amount of resazurin increased from 0.4

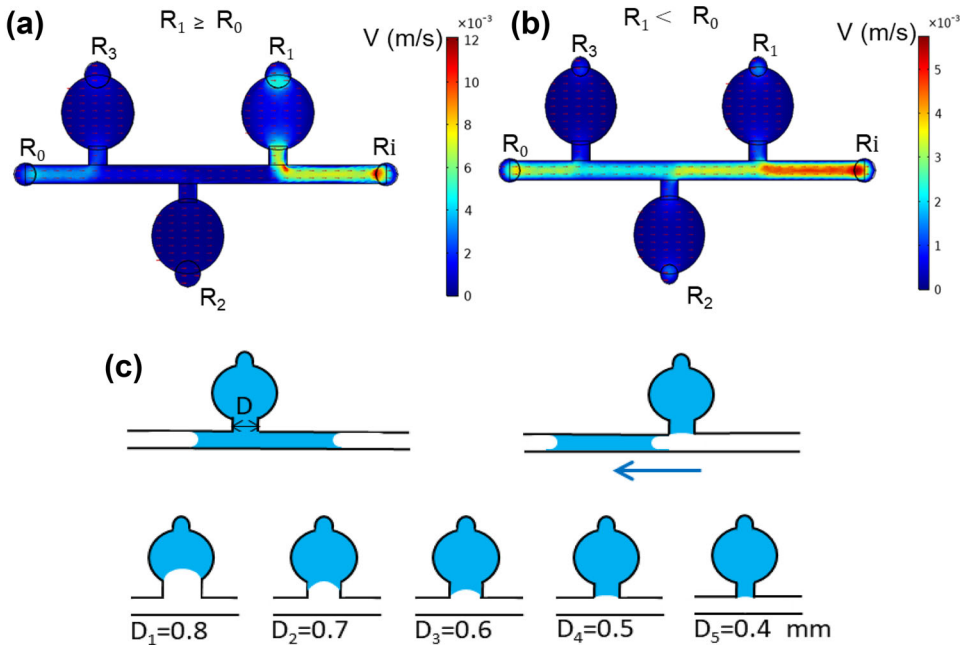

Fig. 2 COMSOL simulation of the gradient concentration and dynamics in the microfluidic chip; the fluid dynamic analysis **a** when $R_1 \geq R_0$; **b** when $R_1 < R_0$; **c** the generated droplets with varying widths of the chamber inlet D

to 2 mg/L. The fluorescence intensity of each image was calculated by subtracting the control intensity from the positive intensity (Fig. 4a) using ImageJ. Based on the result, we chose 0.6 mg/L as the test concentration which has a high signal-to-noise ratio and is a small amount.

On-chip tests of bacterial susceptibility to different antibiotics

To quantify on-chip bacterial growth and MIC, cell growth was measured after culturing for 5 h based on the change in the fluorescence intensity of the culture medium in each chamber as previously recommended in the literature [21, 27], and bacteria were defined as susceptible to antibiotics if the fluorescence intensity of the experimental group (chambers 1 to 11) was decreased by at least 30% compared with the control (chamber 12) [27]. Here, the ratio of fluorescence intensity of each chamber to the control is defined as δ

$$\delta = \mathrm{GV}_i/\mathrm{GV}_{12}, \tag{1}$$

where GV_i and GV_{12} are the fluorescence intensity of each chamber (i.e., chamber 1 to chamber 11) and of chamber 12 after culturing for 5 h, respectively. For instance, a δ value close to one and zero indicates normal bacterial growth and no obvious growth, respectively. In addition, the fluorescence intensity of each of the chambers was determined by ImageJ. According to the recommendation of the Clinical & Laboratory Standards Institute (CLSI), the MIC was defined as the lowest concentration of antibiotics that could thwart bacterial growth [30, 31]. Based on this, we defined two ranges of δ to show the antimicrobial R/S for *E. coli*: $0 < \delta \leq 0.7$ representing "Susceptible" (S), and $\delta > 0.7$ representing "Resistant" (R). The three antibiotics, ampicillin, chloramphenicol, and kanamycin, were used for on-chip AST, and the resulting gradient concentrations were 265.8 ± 18.1, 162.6 ± 5.3, 84.8 ± 10.6, 36.7 ± 6.7, 26.2 ± 5.0, 17.4 ± 1.9, 10.4 ± 2.6, 7.3 ± 2.4, 3.1 ± 1.7, 2.0 ± 0.4, and 1.3 ± 0.3 mg/L for chambers 1 to 11, respectively. For ampicillin, bacteria in chambers 1 to 10 were reported as susceptible (Fig. 5), while in chamber 11, δ was higher than 0.7, which reflected normal bacterial growth. Comparatively, δ values smaller than 0.7 under chloramphenicol treatment suggested that the bacteria were susceptible in chambers 1 to 10. Chamber 11 was reported as resistant ($\delta > 0.7$). Bacteria in chambers 1 to 8 were reported as susceptible, and in chambers 9 to 11 were reported as resistant with kanamycin treatment. We defined the range of MIC as when the value crosses $\delta = 0.7$. As shown in Table 1, the AST results of *E. coli* were overall consistent with results from a conventional 96-well plate with similar MIC values. To conclude, AST with a microfluidic gradient concentration chip shows that *E. coli* MG1655 activities are obviously inhibited by ampicillin (MIC: 2 ± 0.5 mg/L), followed by chloramphenicol (MIC: 2 ± 0.5 mg/L), and kanamycin (MIC: 7.3 ± 2.4 mg/L).

Cell morphological response to ampicillin inhibition

Bacteria may go through morphological changes with the effect of an antibiotic. The bacterial suspension in chambers was taken out and inspected using an optical microscope after culturing for 5 h. In contrast with the lack of morphological change during cell exposure to chloramphenicol and kanamycin, the *E. coli* cells that grew in ampicillin-amended

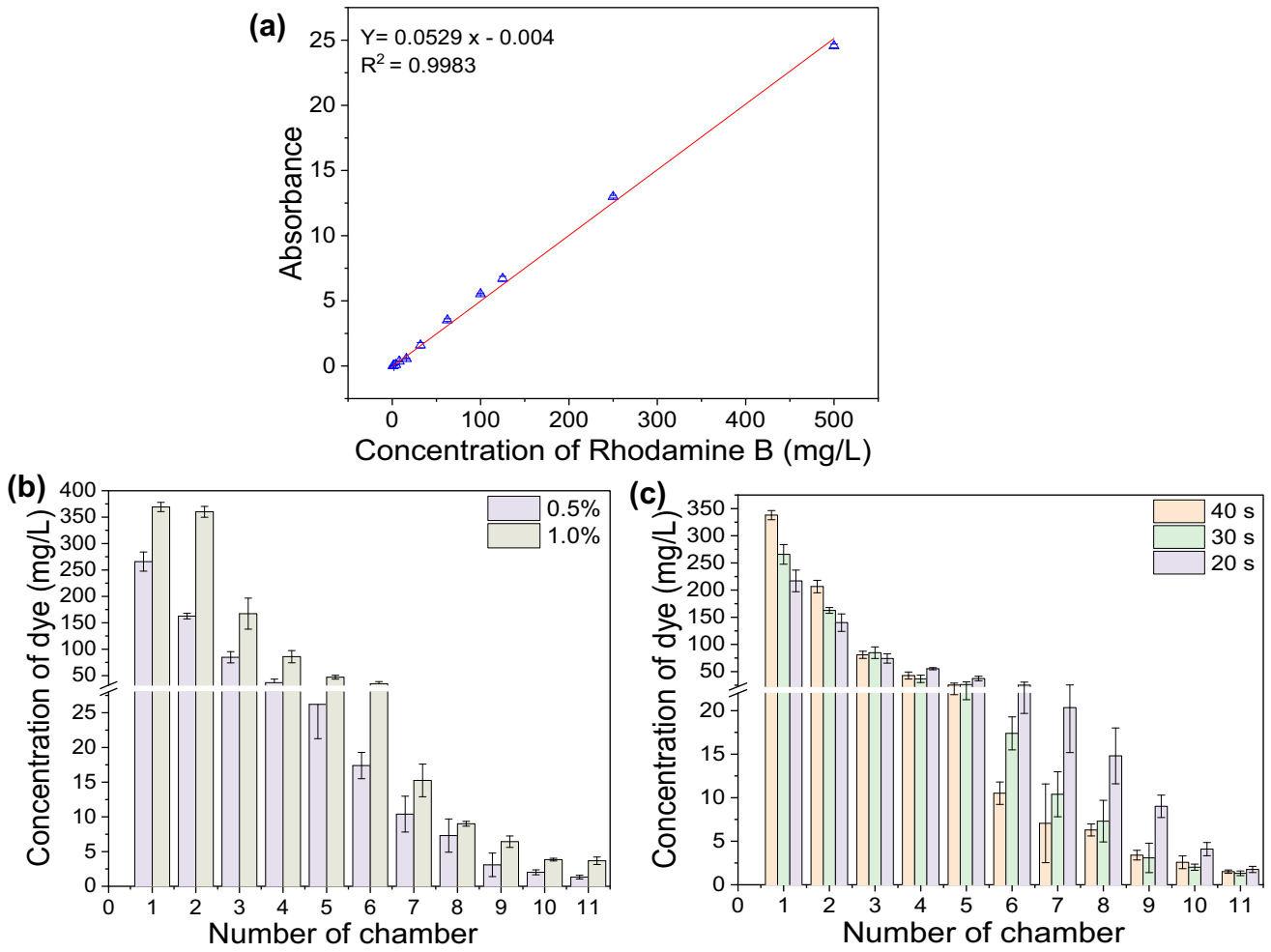

Fig. 3 **a** The calibration curve of rhodamine B concentrations against its absorbance. **b** The generated gradient concentrations with different initial concentrations of rhodamine B. **c** The gradient concentration of rhodamine B with different diffusion times. Error bars indicate the standard deviation of three parallel tests

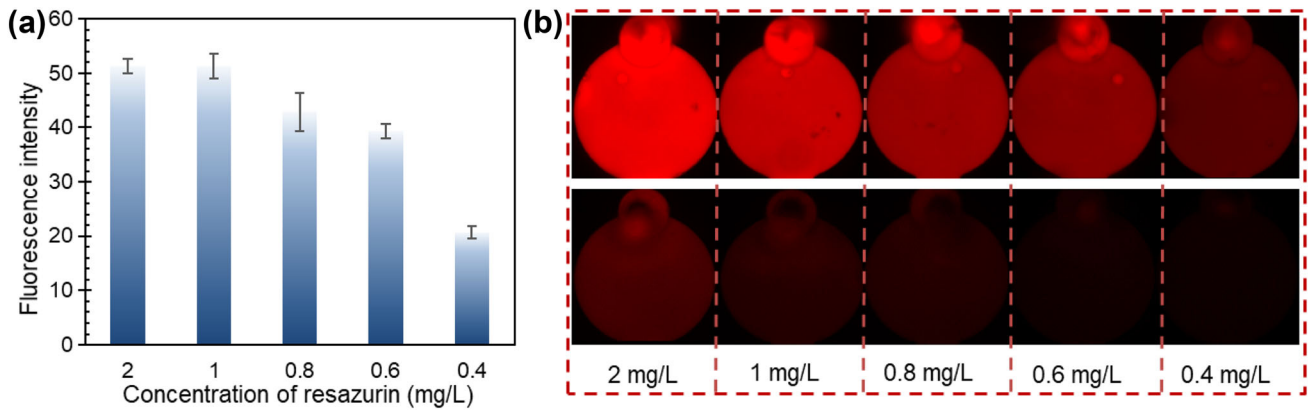

Fig. 4 Fluorescence intensity of five different concentrations of resazurin in the chamber: **a** fluorescence intensity after subtracting the control intensity from the positive intensity; **b** the fluorescence intensity image of the positive group (top: resazurin mixed with bacterial suspension; bottom: resazurin mixed with the culture medium)

Table 1 Comparisons of antibiotic susceptibility and MIC value (mg/L) determined by the microfluidic gradient concentration chip (μGCC) and by conventional 96-well plate assay

Antibiotic	MIC criteria (mg/L) CLSI			MIC (mg/L)		Susceptibility	
	S	I	R	μGCC assay	96-well plate assay	μGCC assay	96-well plate assay
Ampicillin	≤ 8	16	≥ 32	2.0 ± 0.4	2	S	S
Chloramphenicol	≤ 8	16	≥ 32	2.0 ± 0.4	4	S	S
Kanamycin	≤ 16	32	≥ 64	7.3 ± 2.4	8	S	S

S: susceptible; I: intermediate; R: resistant. MIC: minimum inhibitory concentration

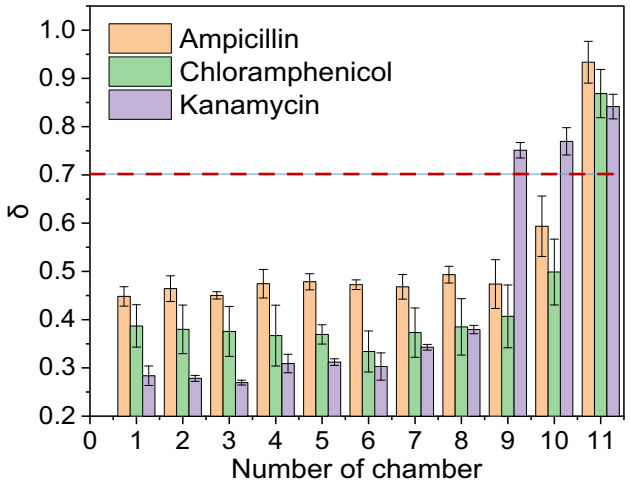

Fig. 5 Influence of different concentrations of antibiotics on the growth of *E. coli*. The dotted horizontal line indicates $\delta = 0.7$

media were found to experience striking filamentous morphological changes in response to ampicillin over time (Fig. 6). We employed the designed concentration gradients across the 12 chip chambers to explore the morphological variations of *E. coli* to ampicillin (Fig. 6). The bacterial cells grew normally in chamber 12 which was set as the control. In chamber 11, bacteria still could propagate, but filamentation of the bacterial cells could be observed. When the concentration was increased from 2.0 ± 0.4 mg/L (chamber 10) to 7.3 ± 2.4 mg/L (chamber 8), longer cells were observed with no obvious propagation. When the concentration continually increased to 10.4 ± 2.4 mg/L (chamber 7) or higher (chambers 6–1), almost no bacterial cells could be observed.

In this study, the gradient concentrations established on our chip provide an operationally simple solution for exploring bacteria cell morphological dynamics exposed to different concentration levels of antibiotics (Fig. 6). This intriguing phenomenon reveals that morphological changes in bacterial cells could be sensitive indicators of antibacterial mechanisms, which in turn could be useful in identifying molecular targets. For example, the dramatic increase in cell length (or filamentation) in our case is most likely induced by ampicillin-targeting of penicillin-binding proteins (PBP) [32]. The β-lactam antibiotic ampicillin can interfere with PBP to inhibit the development of the bacterial cell wall [33]. It has been reported that bacteria can survive by undergoing

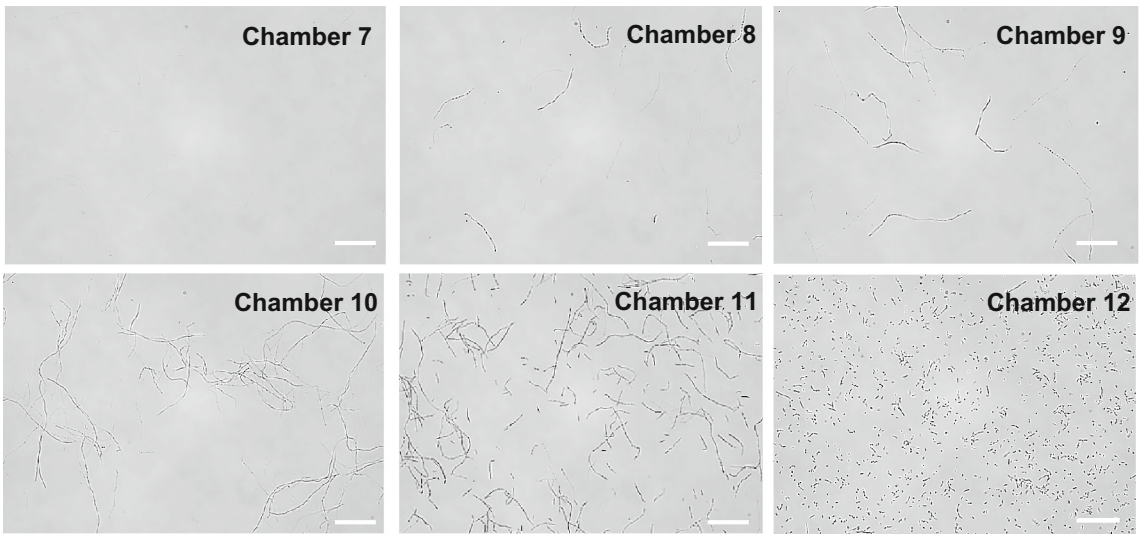

Fig. 6 The inhibitory effect of ampicillin with different concentrations on *E. coli* after 5 h of the on-chip cultivation experiment (scale bar: 50 μm)

antibiotic-induced morphological filamentation [34, 35], as had already been noticed for bacterial cells exposed to other antibiotics, such as amoxicillin [16] and tetracycline [34].

Conclusions

In this study, we report the design and manufacturing of a microfluidic gradient concentration chip equipped with automatic broth dilution for AST using a DLP-based 3D-printing method. DLP-based 3D printing enables the rapid, convenient, and high-precision fabrication of microfluidic devices featuring trapped droplets for independent cell growth. We further demonstrate the optimization of key design parameters of the device including the diffusion time and channel width. Using *E. coli* as the model organism, MIC values determined with three representative antibiotics showed good agreement between on-chip assay and the conventional 96-well plate method. In summary, this microfluidic system provides a simple and robust method for measuring bacterial susceptibility to antibiotics and for exploring potential cell morphological changes in response to antibiotics. The gradient concentration chip presented here provides a proof of concept for rapid AST in clinical settings.

Supplementary Information The online version contains supplementary material available at https://doi.org/10.1007/s42242-021-00173-0.

Acknowledgements The authors would like to thank Mr. Zhuan Ge at Westlake University for providing the suggestions on simulation of fluidic dynamic. This work was supported by the National Natural Science Foundation of China (No. 51908467) and by institutional funds from the Westlake University.

Author contributions FJ, NZ, and HZ conceived the study; HZ designed the project and analyzed the data; YY and YH contributed to methodology and investigation; LZ contributed to the data analysis; HZ and FJ wrote the manuscript; FJ supervised the project. All authors contributed to the proof reading and commenting on the manuscript.

Declarations

Conflict of interest The authors declare that there is no conflict of interest.

Ethical approval This study does not contain any studies with human or animal subjects performed by any of the authors.

References

1. Aslam B, Wang W, Arshad MI et al (2018) Antibiotic resistance: a rundown of a global crisis. Infect Drug Resist 11:1645–1658. https://doi.org/10.2147/IDR.S173867
2. Khan ZA, Siddiqui MF, Park S (2019) Progress in antibiotic susceptibility tests: a comparative review with special emphasis on microfluidic methods. Biotechnol Lett 41(2):221–230. https://doi.org/10.1007/s10529-018-02638-2
3. Zhang T (2020) Rapid antibiotic susceptibility testing platform for direct clinical samples. Honors Scholar Theses 727.
4. Performance Standards for Antimicrobial Susceptibility Testing; Twenty-Third Informational Supplement M100-S23. Clinical and Laboratory Standards Institute, 2013.
5. Matuschek E, Brown DFJ, Kahlmeter G (2014) Development of the EUCAST disk diffusion antimicrobial susceptibility testing method and its implementation in routine microbiology laboratories. Clin Microbiol Infect 20(4):O255–O266. https://doi.org/10.1111/1469-0691.12373
6. Mulroney KT, Hall JM, Huang X et al (2017) Rapid susceptibility profiling of carbapenem-resistant Klebsiella pneumoniae. Sci Rep 7(1):1903–1915. https://doi.org/10.1038/s41598-017-02009-3
7. Aroonnual A, Janvilisri T, Ounjai P et al (2017) Microfluidics: innovative approaches for rapid diagnosis of antibiotic-resistant bacteria. Essays Biochem 61(61):91–101. https://doi.org/10.1042/EBC20160059
8. Churski K, Kaminski TS, Jakiela S et al (2012) Rapid screening of antibiotic toxicity in an automated microdroplet system. Lab Chip 12(9):1629–1637. https://doi.org/10.1039/c2lc21284f
9. Kara V, Duan C, Gupta K et al (2018) Microfluidic detection of movements of Escherichia coli for rapid antibiotic susceptibility testing. Lab Chip 18(5):743–753. https://doi.org/10.1039/C7LC01019B
10. Postek W, Gargulinski P, Scheler O et al (2018) Microfluidic screening of antibiotic susceptibility at a single-cell level shows the inoculum effect of cefotaxime on E. coli. Lab Chip 18(23):3668–3677. https://doi.org/10.1039/C8LC00916C
11. Dai J, Hamon M, Jambovane S (2016) Microfluidics for antibiotic susceptibility and toxicity testing. Bioengineering 3(4):25–37. https://doi.org/10.3390/bioengineering3040025
12. Cira NJ, Ho JY, Dueck ME et al (2020) Combinatorial antimicrobial susceptibility testing enabled by non-contact printing. Micromachines 11(2):142–155. https://doi.org/10.3390/mi11020142
13. Wang X, Liu Z, Pang Y (2017) Concentration gradient generation methods based on microfluidic systems. RSC Adv 7(48):29966–29984. https://doi.org/10.1039/C7RA04494A
14. Zhou B, Gao Y, Tian J et al (2019) Preparation of orthogonal physicochemical gradients on PDMS surface using microfluidic concentration gradient generator. Appl Surface Sci 471:213–221. https://doi.org/10.1016/j.apsusc.2018.11.241
15. Kim SC, Cestellos-Blanco S, Inoue K et al (2015) Miniaturized antimicrobial susceptibility test by combining concentration gradient generation and rapid cell culturing. Antibiotics 4(4):455–466. https://doi.org/10.3390/antibiotics4040455
16. Li B, Qiu Y, Glidle A et al (2014) Gradient microfluidics enables rapid bacterial growth inhibition testing. Anal Chem 86(6):3131–3137. https://doi.org/10.1021/ac5001306
17. Kim S, Lee S, Kim JK et al (2019) Microfluidic-based observation of local bacterial density under antimicrobial concentration gradient for rapid antibiotic susceptibility testing. Biomicrofluidics 13(1):014108. https://doi.org/10.1063/1.5066558
18. Cai LF, Zhu Y, Du GS et al (2012) Droplet-based microfluidic flow injection system with large-scale concentration gradient by a single nanoliter-scale injection for enzyme inhibition assay. Anal Chem 84(1):446–452. https://doi.org/10.1021/ac2029198
19. Keays MC, O'Brien M, Hussain A et al (2016) Rapid identification of antibiotic resistance using droplet microfluidics. Bioengineered 7(2):79–87. https://doi.org/10.1080/21655979.2016.1156824
20. Dewan A, Kim J, McLean RH et al (2012) Growth kinetics of microalgae in microfluidic static droplet arrays. Biotechnol Bioeng 109(12):2987–2996. https://doi.org/10.1002/bit.24568
21. Avesar J, Rosenfeld D, Truman-Rosentsvit M et al (2017) Rapid phenotypic antimicrobial susceptibility testing using nanoliter arrays. Proc Natl Acad Sci 114(29):5787–5795. https://doi.org/10.1073/pnas.1703736114

22. Cira NJ, Ho JY, Dueck ME et al (2012) A self-loading microfluidic device for determining the minimum inhibitory concentration of antibiotics. Lab Chip 12(3):1052–1060. https://doi.org/10.1039/c2lc20887c
23. He Y, Nie J, Xie M et al (2020) Why choose 3D bioprinting? Part III: printing in vitro 3D models for drug screening. Bio-des Manuf 3:160–163. https://doi.org/10.1007/s42242-020-00067-7
24. Yan Q, Dong H, Su J et al (2018) A review of 3D printing technology for medical applications. Engineering 4(5):729–742. https://doi.org/10.1016/j.eng.2018.07.021
25. Mu Q, Wang L, Dunn CK et al (2017) Digital light processing 3D printing of conductive complex structures. Addit Manuf 18:74–83. https://doi.org/10.1016/j.addma.2017.08.011
26. Ali Z, Türeyen EB, Karpat Y et al (2016) Fabrication of polymer micro needles for transdermal drug delivery system using DLP based projection stereo-lithography. Procedia CIRP 42:87–90. https://doi.org/10.1016/j.procir.2016.02.194
27. Azizi M, Zaferani M, Dogan B et al (2018) Nanoliter-sized microchamber/microarray microfluidic platform for antibiotic susceptibility testing. Anal Chem 90(24):14137–14144. https://doi.org/10.1021/acs.analchem.8b03817
28. Sun M, Bithi SS, Vanapalli SA (2011) Microfluidic static droplet arrays with tuneable gradients in material composition. Lab Chip 11(23):3949–1428. https://doi.org/10.1039/c1lc20709a
29. Choi J, Jung YG, Kim J et al (2013) Rapid antibiotic susceptibility testing by tracking single cell growth in a microfluidic agarose channel system. Lab Chip 13(2):280–287. https://doi.org/10.1039/C2LC41055A
30. Lee WB, Fu CY, Chang WH et al (2017) A microfluidic device for antimicrobial susceptibility testing based on a broth dilution method. Biosens Bioelectron 87:669–678. https://doi.org/10.1016/j.bios.2016.09.008
31. Wiegand I, Hilpert K, Hancock RE (2008) Agar and broth dilution methods to determine the minimal inhibitory concentration (MIC) of antimicrobial substances. Nat Protoc 3(2):163–175. https://doi.org/10.1038/nprot.2007.521
32. Cushnie TPT, O'Driscoll NH, Lamb AJ (2016) Morphological and ultrastructural changes in bacterial cells as an indicator of antibacterial mechanism of action. Cell Mol Life Sci 73(23):4471–4492. https://doi.org/10.1007/s00018-016-2302-2
33. Tenover FC (2006) Mechanisms of antimicrobial resistance in bacteria. Am J Med 119(6):S3–S10. https://doi.org/10.1016/j.amjmed.2006.03.011
34. Sun P, Liu Y, Sha J et al (2011) High-throughput microfluidic system for long-term bacterial colony monitoring and antibiotic testing in zero-flow environments. Biosens Bioelectron 26(5):1993–1999. https://doi.org/10.1016/j.bios.2010.08.062
35. Rizzo MG, De Plano LM, Franco D (2020) Regulation of filamentation by bacteria and its impact on the productivity of compounds in biotechnological processes. Appl Microbiol Biotechnol 104:4631–4642. https://doi.org/10.1007/s00253-020-10590-3